

# Continuous Force Decoding from Deep Brain Local Field Potentials for Brain Computer Interfacing

Syed A. Shah<sup>1</sup>, Huiling Tan<sup>1</sup>, Peter Brown<sup>1</sup>

**Abstract**— Current Brain Computer Interface (BCI) systems are limited by relying on neuronal spikes and decoding limited to kinematics only. For a BCI system to be practically useful, it should be able to decode brain information on a continuous basis with low latency. This study investigates if force can be decoded from local field potentials (LFP) recorded with deep brain electrodes located at the Subthalamic nucleus (STN) using data from 5 patients with Parkinson’s disease, on a continuous basis with low latency. A Wiener-Cascade (WC) model based decoder was proposed using both time-domain and frequency-domain features. The results suggest that high gamma band (300-500Hz) activity, in addition to the beta (13-30Hz) and gamma band (55-90Hz) activity is the most informative for force prediction but combining all features led to better decoding performance. Furthermore, LFP signals preceding the force output by up to 1256 milliseconds were found to be predictive of the force output.

## I. INTRODUCTION

A Brain Computer Interface (BCI) is a system that measures brain activity, and processes that to replace, restore, enhance, supplement or improve the natural brain output [1]. A major potential clinical application of BCI is in neural control of limb prostheses to help patients with amputation or paralysis (due to spinal cord injuries, stroke or motor neuron disease e.g. amyotrophic lateral sclerosis). Most existing BCI systems used for prosthetic control are limited to decoding of kinematics only [2]. A neural prosthesis should allow the transduction of both kinematics and force information to enable finer control leading to a better integration in a patient’s life and improved support in daily activities. In addition, most BCI systems are based on processing of neural spikes for decoding movement-related information from the cortex. However, the utility of spike recordings for long-term neural prostheses is limited due to displacements as well as neuronal cell deaths [3]. Surface electrocorticograms (ECoGs) have previously been demonstrated to have greater stability, but only for a few months [4]. Local Field Potentials (LFP) recorded from the Subthalamic nucleus (STN) with deep brain electrodes, on the other hand, have previously been demonstrated to have longevity of at least seven years [5], and could thus offer a more stable and durable signal for BCI systems. In addition, deep brain surgeries for implanting deep brain electrodes are now routinely used for therapeutic reasons and are surgically safe. An alternative option is to explore intra-cortical LFPs. However, intra-cortical LFPs have only been demonstrated to stay stable from 1 [6] to 3 years [7].

Previous evidence suggests that force information is present in the LFP recorded from STN [8]. We had previously shown that we can decode four stages of force development from LFP

[9]. Furthermore, we have recently shown that a model based on low gamma (55-95 Hz) and beta (13-30 Hz) band activities can explain force initiation and holding trajectory on a set of patients [10]. However previous work [9, 10] looked at individual trials which were base-normalized. A practical BCI system should be able to decode the complete force profile as well as correctly decode periods of no force on a continuous basis with acceptable latency to be useful in real-time.

The aim of this study is to investigate if force can be decoded from LFPs recorded from electrodes placed in the STN on a continuous basis with low latency, from Parkinsonian patients. At the time of writing, we are not aware of any other study that has looked into decoding force from deep brain electrodes on a continuous basis, from human subjects. The closest to the work presented in this paper is the work by [11] that decodes force on a continuous basis from human subjects, using ECoGs with medium-density arrays and surface microwire arrays.

## II. METHODS

### A. Experimental Paradigm & Recordings

In this study, patients were instructed to grip a force dynamometer after a visual cue (red light-emitting diode illuminating for 3 seconds) and continue to hold it while the LED stayed on. Patients were given the liberty to randomly choose their own effort level. There were, on average, 31 trials conducted, with each hand in a given session. Both the force dynamometer and LFP recordings were recorded using a TMSi porti (TMS International) amplifier. This paradigm is explained in more detail in [10].

There were 9 patients with idiopathic Parkinson’s disease who had bilateral implantation deemed to have been localized in the STN. All patients gave informed consent and the study was approved by the local ethics committees. The recordings were undertaken 3-6 days after surgery when electrodes were implanted and externalized prior to implantation of a subcutaneous pulse generator. Out of these 18 STNs (from 9 patients), 8 STNs from 5 patients (see Table 1) were selected for further analysis based on fulfilling either of two criteria. First high gamma band (55-95 Hz) synchronization had to be present at movement onset. This is because previous work [10] identified event-related synchronization of gamma band activity (termed as gamma ERS henceforth) to be strongly correlated with the ability to identify force development onset using a first order linear dynamic model. Second patients had to improve with stimulation, as evaluated by the Unified Parkinson’s Disease Rating Scale (UPDRS). This was taken as evidence of satisfactory targeting of the motor STN.

### B. Preprocessing and Feature Extraction

Each electrode had four contact points, labelled as X1-4 where X was either L (left) or R (right). These four monopolar channels were converted into three bipolar channels (by subtracting one from the other), and the best bipolar channel was

These authors are with the MRC Brain Network Dynamics Unit and Nuffield Department of Clinical Neurosciences, University of Oxford, Oxford, OX3 9DU United Kingdom (corresponding author: phone: +44 (0) 1865 234764; e-mail: syed.shah@ndcn.ox.ac.uk).

identified for each STN, based on movement-related beta band desynchronization [10] and used in subsequent analysis. Consecutive 256 millisecond windows, with an overlap of 206 milliseconds were used to extract various time-domain and frequency domain features. This meant that a new feature vector was available every 50 milliseconds. All the LFP channels had a sampling frequency of 2048 Hz.

Table 1: List of selected patients and the STNs that were selected for continuous force decoding based on gamma ERS and clinical assessment

Gender	Age (years)	PD <sup>a</sup> duration (years)	STNs (L:Left, R:Right)	Main symptoms
Male	49	13	L,R	stiffness, bradykinesia, bilateral tremor, freezing
Male	56	10	L,R	bradykinesia, rigidity, tremor, poor gait
Male	56	10	R	Tremor in all four limbs
Female	66	16	L,R	Shuffling, poor balance
Male	52	7	L	Freezing, falls, postural instability, tremor on right side

a PD: Parkinson's disease

*Frequency-domain features:* The identified LFP channel was decomposed into a time-frequency signal by convolving with a complex Morlet wavelet [12]. A linear frequency scale ranging from 0 to 500 Hz (501 frequency points) and a variable number of cycles (4 to 10, varying as a function of frequency) were used in this wavelet transform. Various frequency bands were then identified: 0-4 Hz, 5-7 Hz, 8-12 Hz, 13-20 Hz, 21-30 Hz, 31-45 Hz, 46-55 Hz, 56-95 Hz, 96-105 Hz, 106-200 Hz, 201-300 Hz, 301-349 Hz and 350-500 Hz. The mean power in each of these bands, in a given sliding window was taken as a potential frequency-domain feature.

*Time-domain features:* Similar to the previous work [9], we explored the potential benefit of using additional features derived directly from the time-domain signal. Hjorth proposed three parameters that capture the characteristic of a signal, which are not captured by looking at mean power in specific frequency bands with a wavelet transform [13]. These three features are activity (characterizes the total power of a signal, equivalent to the variance of a signal), mobility (standard deviation of the power spectrum along the frequency axis, equivalent to the standard deviation of the slope of the original signal relative to standard deviation of the signal) and complexity (provides an indication of the smoothness of the signal relative to a sine wave). In addition, the mean value of the LFP signal within a sliding window was identified as a fourth feature (termed as the "mean LFP") similar to the work done in [11].

### C. Wiener Cascade Model

**Figure 1** shows a model that was adopted for decoding force, denoted by  $F(n)$ , from features extracted from the LFPs,  $X(n)$ . The objective is to find the filter coefficients of  $H(z)$  such that the difference between the desired signal ( $F(n)$  denoting force measured from the dynamometer), and the decoded force,  $F'(n)$ , given as output of the filter is minimum in the least squares sense. The input to the filter consists of  $X(n)$  and up to  $N$  lagged versions denoted by convolving  $X(n)$  with  $z^{-k}$  where  $k$  ranges from 1 to  $N$ . Such a filter is called a Wiener filter, and is optimal in the least squares sense. The Wiener filter has traditionally been employed for prediction (where the desired

signal would be a future sample of a signal) and filtering to remove additive noise (where the desired signal would be the original signal, without the additive noise) [14]. Equation (1) represents the predicted force,  $F'(n)$ , as a function of  $M$  features with up to  $N$  lags, where  $x_i(n-j)$  refers to the  $i^{th}$  feature at time corresponding to the  $n^{th}$  sample with a lag of  $j$ . Minimizing the sum of squares of the residuals (difference between the predicted force,  $F'(n)$ , and the desired force,  $F(n)$ ) yields a set of linear equations (called the normal equations) and expressed in matrix form in equation (2) where  $A$  is a  $M(N+1) \times 1$  matrix of  $a_{ij}$ ,  $X$  is a  $P \times M(N+1)$  matrix of all the features, and  $F$  is the  $P \times 1$  vector of actual force where  $P$  is the total number of samples (corresponding to the total number of sliding windows).

$$F'(n) = \sum_{j=0}^N \sum_{i=1}^M a_{ij} x_i(n-j) \quad (1)$$

$$A = (X^T X)^{-1} X^T F \quad (2)$$

$$A = (X^T X + \lambda I)^{-1} X^T F \quad (3)$$

Instead of minimizing only the sum of squares of residuals, a slight modification commonly employed is to add a regularization term ( $A^2$ ) to the residuals. The resulting equation is given by equation (3) where  $\lambda$  is a constant that determines the amount of regularization, and  $I$  is an identity matrix. This is commonly called ridge regression and guards against overfitting.

A limitation of the Wiener filter lies in its inability to model non-linearity. Most systems occurring in nature are non-linear and one solution is to use a Wiener Cascade (WC) filter. This method has previously been used in several studies including decoding of force from ECoG [11]. This involves adjusting the output of the Wiener filter by fitting a high order polynomial (a time-independent, non-linear equation hence called a static non-linearity) to match to the desired output. This is equivalent to minimizing equation (2) where  $E(b_0, b_1, \dots, b_p)$  denotes the error in fitting the  $p^{th}$  order polynomial equation to the output of the Wiener filter,  $F'(n)$ ,  $b_0, b_1, \dots, b_p$  denote the unknown coefficients of the polynomial equation that needs to be determined, and  $F(n)$  is the actual force, and  $N$  is the total number of samples.

$$E(b_0, b_1, \dots, b_p) = \sum_{n=0}^P F(n) - (b_0 + b_1 F'(n) + b_2 (F'(n))^2 + \dots + b_p (F'(n))^p) \quad (4)$$

### D. Cross Validation

In this work,  $k$ -fold cross validation was used. For time-series data, it is important to ensure that continuous chunks of data are used in each fold to ensure that the test part of the signal is independent of the training set. In each iteration,  $k-1$  folds were used for training and validation, and the remaining  $k^{th}$  fold was used for testing. This process was repeated  $k$  times to allow testing on all folds. Consequently, it was possible to test the algorithm on an independent test set to assess the generalization capability of the proposed algorithm. The correlation between the measured force from the dynamometer and the force estimated was computed to assess the performance of the proposed algorithm.

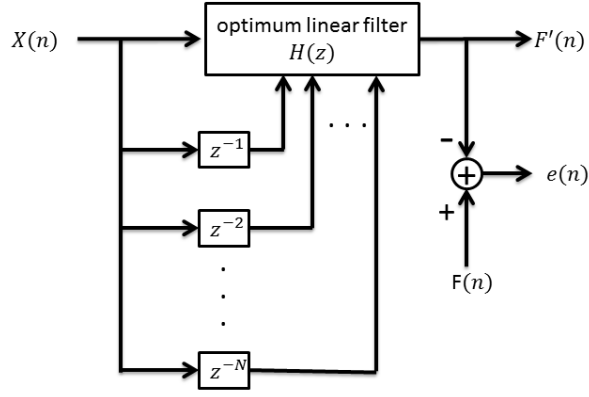


Figure 1 A Wiener filter model, adapted to illustrate how force,  $F'(n)$ , is decoded from features extracted from LFPs,  $X(n)$

### III. RESULTS & DISCUSSION

Figure 2 illustrates force decoding using 4-fold cross validation for a single patient. Notice how each fold is composed of continuous chunks of data (unlike traditional cross-validation techniques, not appropriate for continuous time-series data). In any given iteration, 3 folds are used for training, while the remaining fold is used for testing.

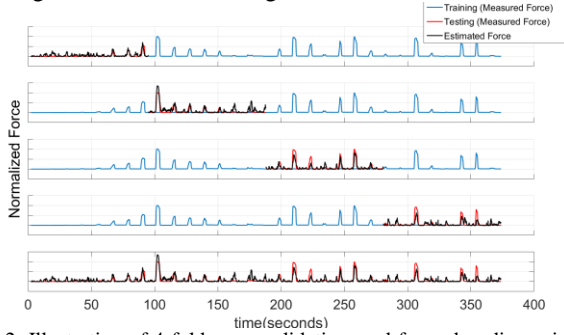


Figure 2: Illustration of 4-fold cross validation, and force decoding using a WC filter with all features at a lag of 40

Table 2: Overall mean and median correlation after applying a Regularized WC filter using all the time-domain and frequency-domain features, with a lag of 40, a polynomial order of 3 and an 11-fold cross validation

PID	Contra-lateral STN (L: Left, R: Right)	Median Correlation	Mean Correlation
1	L	0.75	0.63
1	R	0.82	0.71
2	L	0.30	0.26
2	R	0.71	0.57
3	L	0.63	0.63
4	L	0.56	0.57
4	R	0.54	0.47
5	R	0.61	0.57

Table 2 shows the median correlation (median of 11 folds) and the mean correlation of all the 8 STNs from 5 patients, with a Regularized WC filter using all the time-domain and frequency-domain features, a lag of 40, and a polynomial order of 3 for the static non-linearity. Figure 3 shows the scatter plot of the median correlation (median from each testing fold) for each patient, against gamma ERS and it can be seen that gamma ERS correlates strongly with algorithm performance. Consequently, further analysis is carried out using only the 5 STNs from 3

patients who had high gamma ERS and the best performance overall. We investigated the need for cascading a static non-linearity with a standard Wiener filter, the variation of performance with amount of lag, the order of the polynomial of the non-linearity, and the presence of any potential improvement by adding more features in comparison with using only beta (13-30 Hz) and gamma bands (55-95 Hz) as was done in [10], previously.

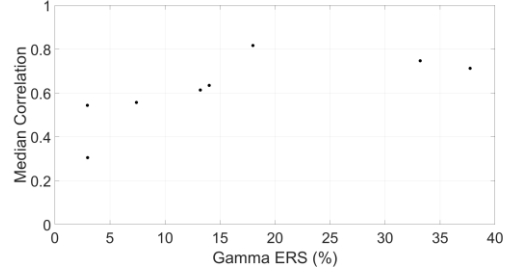


Figure 3: Median correlation against gamma ERS, after using a Regularized WC filter, with a lag of 40, a polynomial order of 3, and 11-fold cross validation

Figure 4 shows the mean error after using only a Wiener filter and after cascading a static non-linearity of 3<sup>rd</sup> order, with all lags from 0 to 50. It can be seen that adding a static non-linearity improves force decoding, and best performance seems to be achieved with a lag of around 20 (corresponding to using features from previous windows for up to 1256 milliseconds).

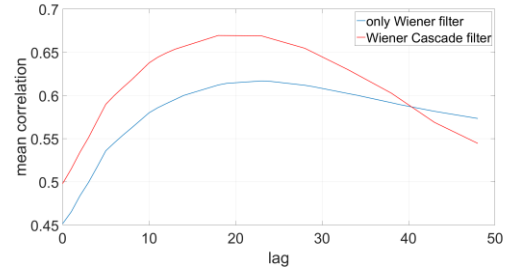


Figure 4: Performance variation with different amounts of lag, using only a Wiener filter and a WC filter with a 3rd order polynomial

Figure 5 shows the variation of mean error across the 5 STNs, with different polynomial order, from 1 to 10. It can be seen that using a 4<sup>th</sup> order polynomial gives the best prediction performance.

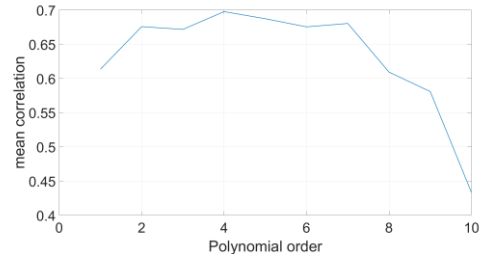


Figure 5: Performance variation with polynomial order chosen for the static non-linearity

Figure 6 shows the mean and standard deviation of correlation when different features are added in addition to beta (13-30Hz) and gamma (55-95Hz). The figure suggests that high gamma band (300-500Hz) activity was the single feature providing the most improvement, but that using all the features together lead to even greater improvement, with low variance.

While a neural network might be considered a more suitable approach for building a non-linear decoder, it is prone to

overfitting and requires techniques like early stopping (based on validation error) or heavy regularization to penalize large weights. Using more layers in a neural network, it is possible to create a force decoder which is at least as good as the WC filter, but it becomes increasingly likely to overfit with increasing complexity of the network architecture. Figure 7 shows a specific example of using a (17-10-1) network on a single patient showing the mean correlation with different amounts of regularization. For reference, the mean correlation obtained after using a CW model is also shown. It can be seen that low regularization leads to overfitting (high variance) and hence worse performance than CW-based force decoding. However, as the amount of regularization is increased, the mean correlation on the test set starts improving and becomes better than CW. As expected, further regularization leads to decreasing performance suggesting over-regularization (high bias). Determining the optimal amount of regularization with a neural network is computationally far more expensive than CW-based decoding, as the optimal amount of regularization will vary from patient to patient and the additional gain in performance is minimal. This is likely because any non-linearity is already captured by the static non-linearity part of the CW model thereby obviating the need for using more computationally expensive techniques like neural networks.

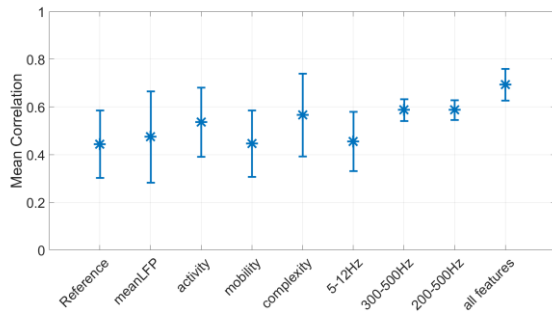


Figure 6: Every feature added leads to improvement, and hence it is best to use all available features

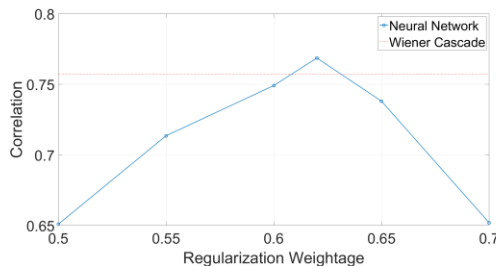


Figure 7: Both under and over-regularized neural network models lead to poor performance, the former due to high variance and the latter due to high bias

Lastly the force decoding performance was significantly better on the contra-lateral side than the ipsi-lateral side ( $0.61 \pm 0.19$  as opposed to  $0.37 \pm 0.35$ ) for the 5 STNs shortlisted, using a specific lag, and polynomial order.

There are a number of reasons that make it unlikely that movement artefact was responsible for the force decoding demonstrated in this work. Firstly, the force applied was isometric thereby minimizing any artefactual movement during the experiment. Secondly, the decoding performance improved with lag suggesting that features derived from signals from STN recorded prior to actual force output were involved in decoding

force. Thirdly, a movement artefact is likely to result in wideband power across the whole frequency spectrum, not observed in our study. Furthermore, this work is not decoding only specific segments of experiment where a patient is gripping with force but the entire duration while the patient is undertaking the experiment. Lastly, there is a significant difference in force decoding performance using contra-lateral STN as opposed to ipsi-lateral STN, which is consistent with our understanding that, anatomically, STN is lateralized.

#### IV. CONCLUSION

We are not aware of any previous study that has shown continuous decoding of force from local field potentials, recorded from deep cortical structures in human subjects. Furthermore, we have shown that there is benefit to using more features, in addition to the selected beta and low gamma bands, and even further improvement when more time-domain features are selected. There is a non-linearity which can be captured by cascading the Wiener filter with a static non-linearity. There is very little benefit to using neural networks to decode force, at the cost of significant computational complexity. A WC filter offers a fast algorithm for decoding force, and it is able to handle non-linear relationships obviating the need for other non-linear but computationally more expensive techniques. Future work will involve using the proposed method to decode force in real-time providing feedback (of the decoded force) to the patient. We believe that the method proposed in this work is fast enough to allow decoding at low latencies and can thus be used for online force decoding. This is likely to have significant implication for developing BCI systems allowing more fine-tuning of outputs, controlled by LFP signals from deep cortical structures (STN).

#### REFERENCES

1. Wolpaw, J. and E.W. Wolpaw, *Brain-computer interfaces: principles and practice*. 2012: OUP USA.
2. Collinger, J.L., et al., *High-performance neuroprosthetic control by an individual with tetraplegia*. The Lancet, 2013. **381**(9866): p. 557-564.
3. Hall, T.M., K. Nazarpour, and A. Jackson, *Real-time estimation and biofeedback of single-neuron firing rates using local field potentials*. Nature communications, 2014. **5**.
4. Chao, Z.C., Y. Nagasaka, and N. Fujii, *Long-term asynchronous decoding of arm motion using electrocorticographic signals in monkey*. Frontiers in neuroengineering, 2010. **3**: p. 3.
5. Giannicola, G., et al., *Subthalamic local field potentials after seven-year deep brain stimulation in Parkinson's disease*. Experimental neurology, 2012. **237**(2): p. 312-317.
6. Flint, R.D., et al., *Long term, stable brain machine interface performance using local field potentials and multiunit spikes*. Journal of neural engineering, 2013. **10**(5): p. 056005.
7. Flint, R.D., et al., *Long-term stability of motor cortical activity: implications for brain machine interfaces and optimal feedback control*. Journal of Neuroscience, 2016. **36**(12): p. 3623-3632.
8. Anzak, A., et al., *Subthalamic nucleus activity optimizes maximal effort motor responses in Parkinson's disease*. Brain, 2012: p. aws183.
9. Shah, S.A., H. Tan, and P. Brown, *Decoding force from deep brain electrodes in Parkinsonian patients*. In Engineering in Medicine and Biology Society (EMBC), 2016 IEEE 38th Annual International Conference of the. 2016. IEEE.
10. Tan, H., et al., *Decoding gripping force based on local field potentials recorded from subthalamic nucleus in humans*. eLife, 2016. **5**: p. e19089.
11. Flint, R.D., et al., *Extracting kinetic information from human motor cortical signals*. NeuroImage, 2014. **101**: p. 695-703.
12. Cohen, M.X., *Analyzing neural time series data: theory and practice*. 2014: MIT Press.
13. Hjorth, B., *EEG analysis based on time domain properties*. Electroencephalography and clinical neurophysiology, 1970. **29**(3): p. 306-310.
14. Proakis, J.G. and D.G. Manolakis, *Digital Signal Processing: Principles, Algorithms, and Applications*. 1996: Prentice Hall.